

# Low temperature vortex liquid in $\text{La}_{2-x}\text{Sr}_x\text{CuO}_4$

Lu Li<sup>1</sup>, J. G. Checkelsky<sup>1</sup>, Seiki Komiya<sup>2</sup>, Yoichi Ando<sup>2</sup>, and N. P. Ong<sup>1\*</sup>

<sup>1</sup>Department of Physics, Princeton University, Princeton, NJ 08544, USA

<sup>2</sup>Central Research Institute of Electric Power Industry, Komae, Tokyo 201-8511, Japan

(Dated: April 16, 2018)

In the cuprates, the lightly-doped region is of major interest because superconductivity, antiferromagnetism, and the pseudogap state [1, 2, 3] come together near a critical doping value  $x_c$ . These states are deeply influenced by phase fluctuations [4] which lead to a vortex-liquid state that surrounds the superconducting region [5, 6]. However, many questions [7, 8, 9, 10, 11] related to the nature of the transition and vortex-liquid state at very low temperatures  $T$  remain open because the diamagnetic signal is difficult to resolve in this region. Here, we report torque magnetometry results on  $\text{La}_{2-x}\text{Sr}_x\text{CuO}_4$  (LSCO) which show that superconductivity is lost at  $x_c$  by quantum phase fluctuations. We find that, in a magnetic field  $H$ , the vortex solid-to-liquid transition occurs at field  $H_m$  much lower than the depairing field  $H_{c2}$ . The vortex liquid exists in the large field interval  $H_m \ll H_{c2}$ , even in the limit  $T \rightarrow 0$ . The resulting phase diagram reveals the large fraction of the  $x$ - $H$  plane occupied by the quantum vortex liquid.

In underdoped LSCO, the magnetic susceptibility is dominated by the Curie-like spin susceptibility and the van Vleck orbital susceptibility [14, 15]. These large paramagnetic contributions render weak diamagnetic signals extremely difficult to detect using standard magnetometry in lightly-doped crystals. However, because the spin susceptibility is nearly isotropic [16] while the incipient diamagnetism is highly anisotropic (the supercurrents are in-plane), torque magnetometry has proved to be effective in resolving the diamagnetic signal [12, 13, 17, 18]. With  $\mathbf{H}$  tilted at a slight angle  $\phi$  to the crystal  $c$ -axis, the torque  $\tau$  may be expressed as an effective magnetization  $M_{obs} \equiv \tau/\mu_0 H_x V$ , where  $V$  is the sample volume,  $\mu_0$  the permeability and  $H_x = H \sin \phi$  (we take  $\hat{\mathbf{z}} \parallel \hat{\mathbf{c}}$ ). In cuprates,  $M_{obs}$  is comprised of 3 terms [12, 13]

$$M_{obs}(T, H_z) = M_d(T, H_z) + \Delta M_s(T, H_z) + \Delta \chi^{orb}(T) H_z, \quad (1)$$

where  $M_d(T, H_z)$  the diamagnetic magnetization of interest,  $\Delta M_s$  the anisotropy of the spin local moments, and  $\Delta \chi^{orb}$  the anisotropy of the van Vleck orbital susceptibility [see SI]. Hereafter, we write  $H$  for  $H_z$ .

We label the 7 samples studied as 03 (with  $x = 0.030$ ), 04 (0.040), 05 (0.050), 055 (0.055) 06 (0.060), 07 (0.070) and 09 (0.090). To start, we confirmed that, above  $\sim 25$  K,  $M_{obs}$  derived from the torque experiment in sample 03 is in good, quantitative agreement with the anisotropy

inferred from previous bulk susceptibility measurements on a large crystal of LSCO ( $x = 0.03$ ) [16] (see SI for comparisons).

Figure 1 displays the magnetization  $M_{obs}$  in samples 055 and 06. The pattern of  $M_{obs}$  results from the sum of the 3 terms in Eq. 1. Panel (a) shows how it evolves in sample 055. At high  $T$  (60–200 K), the curves of  $M_{obs}$  vs.  $H$  are fan-like, reflecting the weak  $T$  dependence of the orbital term  $\Delta \chi^{orb}(T) H$  [12]. At the onset temperature for diamagnetism  $T_{onset}$  (55 K, bold curve), the diamagnetic term  $M_d$  appears as a new contribution. The strong  $H$  dependence of  $M_d$  causes  $M_{obs}$  to deviate from the  $H$ -linear behavior. In Panel b, the evolution is similar, except that the larger diamagnetism forces  $M_{obs}$  to negative values at low  $H$ . As mentioned, the spin contribution  $\Delta M_s$  is unresolved above  $\sim 40$  K in both panels. To magnify the diamagnetic signal, it is convenient to subtract the orbital term  $\Delta \chi_{orb} H$ .

The resulting curves  $M'_{obs}(T, H) \equiv M_{obs} - \Delta \chi^{orb} H$  are shown for sample 05 in Panel (c). At low fields  $M'_{obs}$  displays an interesting oscillatory behavior (curves at 0.5 and 0.75 K), but at high fields it tends towards saturation. By examining how  $M'_{obs}$  behaves in the 2 limits of weak and intense fields in the 7 samples (see SI), we have found that  $M'_{obs}$  is comprised of a diamagnetic term  $M_d(T, H)$ , that closely resembles the “tilted hill” profile of diamagnetism in the vortex liquid state above the critical temperature  $T_c$  reported previously [6, 12], and a spin-anisotropy term  $\Delta M_s$  that becomes large at low  $T$ . Modeling the latter as free spin- $\frac{1}{2}$  local moments with anisotropic  $g$  factors measured with  $\mathbf{H} \parallel \mathbf{c}$  ( $g_c$ ) and  $\mathbf{H} \perp \mathbf{c}$  ( $g_{ab}$ ), we have (details in SI)

$$\Delta M_s(T, H) = \mathcal{P}(T) \tanh[\beta g_\phi \mu_B B/2], \quad (2)$$

with  $\mu_B$  the Bohr magneton,  $\beta = 1/k_B T$  and  $g_\phi = \sqrt{(g_c \cos \phi)^2 + (g_{ab} \sin \phi)^2}$ . With  $g_\phi \sim g_c$  fixed at 2.1, the sole adjustable parameter at each  $T$  is the prefactor  $\mathcal{P}(T)$ .

Equation 2 accounts very well for the curves in Fig. 1c, especially the oscillatory behavior and the saturation at large  $H$ : at  $T = 0.5$  and 0.75 K,  $\Delta M_s \sim 1/k_B T$  dominates  $M_d$  in weak  $H$ , but for  $H > k_B T/g_c \mu_B$ , the saturation of  $\Delta M_s$  implies that  $M'_{obs}(H)$  adopts the profile of  $M_d(H)$  apart from a vertical shift. Lightly doped LSCO enters a spin- or cluster-glass state [14, 15] below the spin-glass temperature  $T_{sg}$  which is sensitive to sample purity (in our crystals 03 and 04,  $T_{sg} \sim 2.5$  and 1 K, respectively). The magnetic hysteresis below  $T_{sg}$  (clockwise) is distinct from the hystereses (anticlockwise) in the vortex solid, and is significant in only these 2 samples.

\*preprint submitted to Nature Physics

Subtracting  $\Delta M_s$  from  $M'_{obs}$ , we isolate the purely diamagnetic term  $M_d(T, H)$ . In Fig. 2, we display the curves of  $M_d$  and  $\Delta M_s$  at selected  $T$  in samples 04, 05, 055 and 06. The samples 03, 04 and 05 do not display any Meissner effect at all. The strict reversibility of the  $M_d$ - $H$  curves confirms that we are in the vortex-liquid state in 03, 04 and 05. When  $x$  exceeds  $x_c$ , the samples display broad Meissner transitions ( $T_c \sim 0.5$  and 5 K in 055 and 06, respectively). Hysteretic behavior appears below a strongly  $T$ -dependent irreversibility field  $H_{irr}(T)$ , which we discuss shortly. Examination of the  $T$  dependences in the 4 panels uncovers an important pattern. In the vortex liquid, the overall magnitude of  $M_d$  grows rapidly as we cool from 35 to 5 K, but it stops changing below a crossover temperature  $T_Q$  ( $\sim 4$  K in samples 05, 055 and 06, and  $\sim 2$  K in 04). Even in 06, where  $H_{irr} \sim 9$  T at 0.35 K,  $M_d$  recovers the  $T$ -independent profile when  $H > H_{irr}$  (note the diverging branches at 9 T in Panel d). The insensitivity to  $T$  suggests that the excitations, which degrade the diamagnetic response in the liquid state, are governed by quantum statistics below  $T_Q$ .

In intense fields, the field suppression of  $M_d$  provides an estimate of the depairing field  $H_{c2}$  ( $\sim 20, 25, 35, 43$ , and 48 T in samples 03, 04, 05, 055, and 06, respectively). We find that  $H_{c2}$  is nominally  $T$ -independent as reported earlier [12].

Experimentally, the appearance of hysteresis in  $M_d$  vs.  $H$  below  $H_{irr}(T)$  is a sensitive barometer of the vortex solid. The strong vortex pinning in LSCO leads to large hystereses as soon as the vortex system exhibits shear rigidity. The hysteretic loops, which appear in 055 expand very rapidly as  $x$  exceeds 0.055. By plotting the hysteretic loops in magnified scale (Fig. 3a shows curves for 06), we can determine  $H_{irr}(T)$  quite accurately. Vortex avalanches – signatures of the vortex solid – are observed (for  $H < H_{irr}$ ) unless the field-sweep rate is very slow (see SI).

The temperature dependence of  $H_{irr}(T)$  is plotted in Fig. 3b for samples  $x > x_c$ . At low  $T$ , the dependence approaches the exponential form

$$H_{irr}(T) = H_0 \exp(-T/T_0). \quad (3)$$

The parameters  $H_0$  and  $T_0$  decrease steeply as  $x \rightarrow x_c$ . Previous experiments in cuprates were not performed to low enough  $T$  or to high enough  $H$  to observe the exponential form. The field parameter  $H_0$  provides an upper bound for the zero-Kelvin melting field  $H_m(0)$  (at some  $T < 0.35$  K, crossover to a quantum melting may cause  $H_{irr}$  to deviate from Eq. 3, so  $H_0$  here is a close upper bound to  $H_m(0)$ ). Equation 3 is reminiscent of the Debye-Waller factor, and strongly suggests that the excitations responsible for the melting transition follow classical statistics at temperatures down to 0.35 K. The classical nature of these excitations contrasts with the quantum nature of the excitations in the vortex liquid below  $T_Q$  described above.

The inferred values of  $H_0$  (2, 13, 25 and 40 T in 055, 06,

07, and 09, respectively) are much smaller than  $H_{c2}(0)$ . Hence, after the vortex solid melts, there exists a broad field range in which the vortices remain in the liquid state at low  $T$ . The existence of the liquid at  $T < T_Q$  implies very large zero-point motion associated with a small vortex mass  $m_v$ , which favors a quantum-mechanical description.

Finally, we construct the low- $T$  phase diagram in the  $x$ - $H$  plane. Figure 4 shows that the  $x$  dependence of  $H_{c2}(0)$ , the depairing field scale, is qualitatively distinct from that of  $H_0$ , the boundary of the vortex solid. The former varies roughly linearly with  $x$  between 0.03 and 0.07 with no discernible break-in-slope at  $x_c$ , whereas  $H_0$  falls steeply towards zero at  $x_c$  with large negative curvature. This sharp decrease – also reflected in the 1000-fold shrinkage of the hysteresis amplitude between  $x = 0.07$  and 0.055 – is strong evidence that the collapse of the vortex solid is a quantum critical transition. This is shown by examining the variation of  $H_{irr}$  vs.  $x$  at several fixed  $T$  (dashed lines). At 4 K,  $H_{irr}$  approaches 0 gently with positive curvature, but at lower  $T$ , the trajectories tend towards negative curvature. In the limit  $T = 0$ ,  $H_0$  approaches zero at  $x_c$  with nearly vertical slope. The focussing of the trajectories to the point  $(x_c, 0)$  is characteristic of a sharp transition at  $x_c$ , and strikingly different from the smooth decay suggested by viewing lightly-doped LSCO as a system of superconducting islands with a broad distribution of  $T_c$ 's.

In Fig. 4 the high-field vortex liquid is seen to extend continuously to  $x < x_c$  where it co-exists with the cluster/spin-glass state [14, 15] (samples 03, 04 and 05). As shown in Fig. 2 (see SI), the robustness of  $M_d$  to intense fields attests to unusually large pairing energy even at  $x = 0.03$ , but the system stays as a vortex liquid down to 0.35 K.

In the limit  $H \rightarrow 0$ , the vortex liquid ( $x < x_c$ ) has equal populations of vortices and antivortices. This implies that, if  $x$  is reduced below  $x_c$  at low  $T$  and in zero field, superconductivity is destroyed by the spontaneous appearance of free vortices and antivortices engendered by increased charge localization and strong phase fluctuation [7, 8, 10]. The experiment lends support to the picture that, at  $T = 0$  in zero field, superconductivity first transforms to a vortex-liquid state that has strong pairing but lacks phase coherence before the insulating state is attained. The rapid growth of the spin/cluster-glass state in LSCO suggests that incipient magnetism also plays a role in destroying superconductivity. In summary, we find that the pair condensate in LSCO is robust even for  $x = 0.03$  in fields of 25 T and higher. However, because the vortex solid melts at a lower field  $H_0$ , the condensate exists as a vortex liquid that resists solidification down to 0.35 K, implying large zero-point motion consistent with a small vortex mass. In the phase diagram (Fig. 4), the vortex liquid surrounds the vortex solid region. The evidence supports a sharp quantum critical transition at  $x_c$ . However, the  $T$  dependence in Eq. 3 implies that the quantum melting of the solid must

occur below 0.35 K even as  $x \rightarrow x_c$ .

**Acknowledgements** Valuable discussions with Yayu Wang, Z. Tešanović, S. Sachdev, S. A. Kivelson, P. W. Anderson and J. C. Davis are acknowledged. The research at Princeton was supported by the National Science Foundation (NSF) through a MRSEC grant DMR

0213706. Research at CRIEPI was supported by a Grant-in-Aid for Science from the Japan Society for the Promotion of Science. The high field measurements were performed in the National High Magnetic Field Lab. Tallahassee, which is supported by NSF, the Department of Energy and the State of Florida.

---

[1] For a review, see Timusk, T. and Statt, B., The pseudogap in high-temperature superconductors: an experimental survey, *Rep. Prog. Phys.* **62**, 61-122 (1999).

[2] Lee, P. A., Nagaosa, N., Wen X. G., Doping a Mott insulator: Physics of high-temperature superconductivity, *Rev. Mod. Phys.* **78**, 17-85 (2006).

[3] Anderson, P. W., Present status of the theory of the high- $T_c$  cuprates, *Low Temperature Physics* **32**, 282-289 (2006).

[4] Emery, V. J. and Kivelson, S. A., Importance of phase fluctuations in superconductors with small superfluid density, *Nature* **374**, 434 - 437 (1995).

[5] Wang, Y. *et al.*, The onset of the vortex-like Nernst signal above  $T_c$  in  $\text{La}_{2-x}\text{Sr}_x\text{CuO}_4$  and  $\text{Bi}_{2}\text{Sr}_{2-y}\text{La}_y\text{CuO}_6$ , *Phys. Rev. B* **64**, 224519 (2001).

[6] Wang, Y., Li, L., and Ong, N. P., Nernst effect in high- $T_c$  superconductors, *Phys. Rev. B* **73**, 024510 (2006).

[7] Doniach, S., Quantum fluctuations in two-dimensional superconductors, *Phys. Rev. B* **24**, 5063 (1981).

[8] Fisher, M. P. A., Weichman, P. B., Grinstein, G. and Fisher, D. S., Boson localization and the superfluid-insulator transition, *Phys. Rev. B* **40**, 546 (1989).

[9] Fisher, M. P. A. and Lee, D. H., Correspondence between two-dimensional bosons and a bulk superconductor in a magnetic field, *Phys. Rev. B* **39**, 2756 (1989).

[10] Melikyan, A. and Tešanović, Z., A model of phase fluctuations in a lattice  $d$ -wave superconductor: application to the Cooper pair charge-density-wave in underdoped cuprates, *Phys. Rev. B* **71**, 214511 (2005).

[11] Nikolić, P. and Sachdev, S., Effective action for vortex dynamics in clean  $d$ -wave superconductors, *Phys. Rev. B* **73**, 134511 (2006).

[12] Wang, Y. *et al.*, Field-enhanced diamagnetism in the pseudogap state of the cuprate  $\text{Bi}_2\text{Sr}_2\text{CaCu}_2\text{O}_{8+\delta}$  superconductor in an intense magnetic field, *Phys. Rev. Lett.* **95**, 247002 (2005).

[13] Li, L. *et al.*, Strongly nonlinear magnetization above  $T_c$  in  $\text{Bi}_2\text{Sr}_2\text{CaCu}_2\text{O}_{8+\delta}$ , *Eurpophys. Lett.* **72**, 451-457 (2005).

[14] Keimer, B. *et al.*, Magnetic excitations in pure, lightly doped, and weakly metallic  $\text{La}_2\text{CuO}_4$ , *Phys. Rev. B* **46**, 14034 (1992).

[15] Niedermayer, Ch., Bernhard, C., Blasius, T., Golnik, A., Moodenbaugh, A. and Budnick, J. I., Common Phase Diagram for Antiferromagnetism in  $\text{La}_{2-x}\text{Sr}_x\text{CuO}_4$  and  $\text{Y}_{1-x}\text{Ca}_x\text{Ba}_2\text{CuO}_6$  as Seen by Muon Spin Rotation, *Phys. Rev. Lett.* **80**, 3843 (1998).

[16] Liovov, A. N., Ando, Y., Komiya, S. and Tsukada, I., Unusual Magnetic Susceptibility Anisotropy in Untwinned  $\text{La}_{2-x}\text{Sr}_x\text{CuO}_4$  Single Crystals in the Lightly Doped Region, *Phys. Rev. Lett.* **87**, 017007 (2001).

[17] D. E. Farrell *et al.*, Experimental evidence for a transverse magnetization of the Abrikosov lattice in anisotropic superconductors, *Phys. Rev. Lett.* **61**, 2805-2808 (1988).

[18] Bergemann, C. *et al.*, Superconducting magnetization above the irreversibility line in  $\text{Tl}_2\text{Ba}_2\text{CuO}_{6+\delta}$ , *Phys. Rev. B* **57**, 14387 (1998).

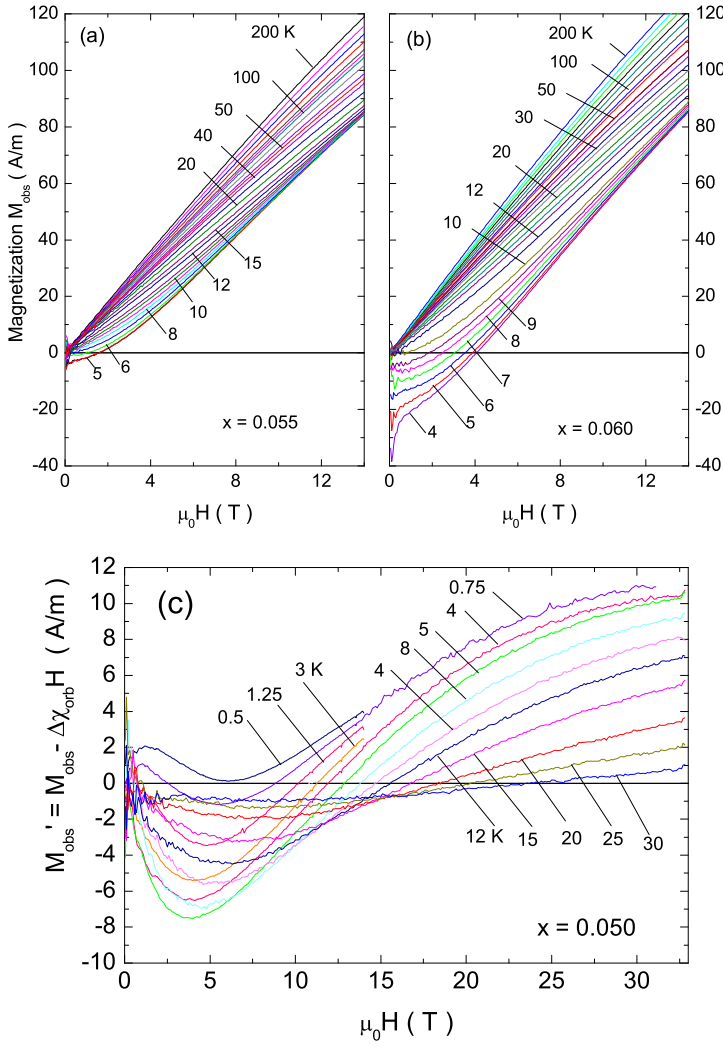


FIG. 1: Curves of the observed magnetization  $M_{obs}$  vs.  $H$  at temperatures 4–200 K in sample 055 (Panel a,  $T_c \sim 0.5$  K) and 06 (Panel b,  $T_c \sim 5$  K). The crystal is glued to the tip of the cantilever with its  $c$ -axis at a small angle  $\phi \sim 15^\circ$  to the field  $\mathbf{H}$ . Above  $T_{onset}$  (bold curves at 55 and 70 K in a and b, respectively), the fan-like pattern is due entirely to the paramagnetic term  $\Delta\chi^{orb}(T)H$  (see SI for plot of  $\Delta\chi(T)$ ). Below  $T_{onset}$ , the diamagnetic term  $M_d$  becomes evident. Panel (c) shows the profiles of  $M'_{obs} = M_{obs} - \Delta\chi^{orb}H$  in the sample 05. Note the oscillation in weak  $H$  at  $T = 0.5$  and 0.75 K and the approach towards saturation in high fields. These curves are separated into  $\Delta M_s$  and  $M_d$  in Fig. 2b.

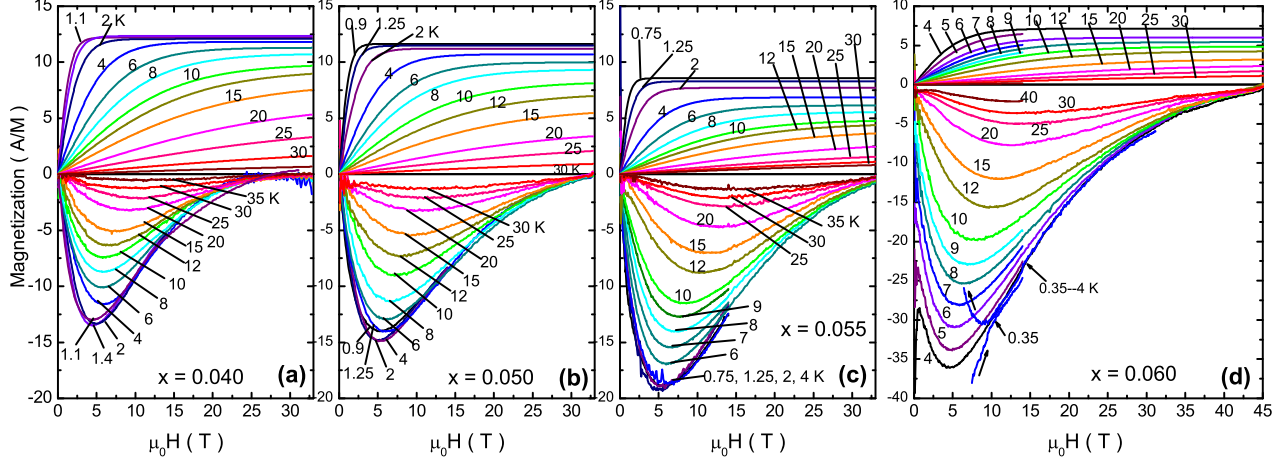


FIG. 2: The paramagnetic spin term  $\Delta M_s(T, H)$  and the diamagnetic term  $M_d(T, H)$  vs.  $H$  in samples 04, 05, 055 and 06 (Panels a–d, respectively). In each panel, the diamagnetic minimum (at 5 T) deepens rapidly between 30 K and 5 K, but ceases to change below  $T_Q$ . The depairing field  $H_{c2}$  is estimated to be 25, 35, 43, and 48 T in Panels (a)–(d), respectively. In Panel d, the branching curves (with arrows) indicate the high-field limit of the vortex solid at 0.35 K. Above  $H_{irr}(T)$ , the low- $T$  curves merge with the vortex-liquid curve at 4 K.

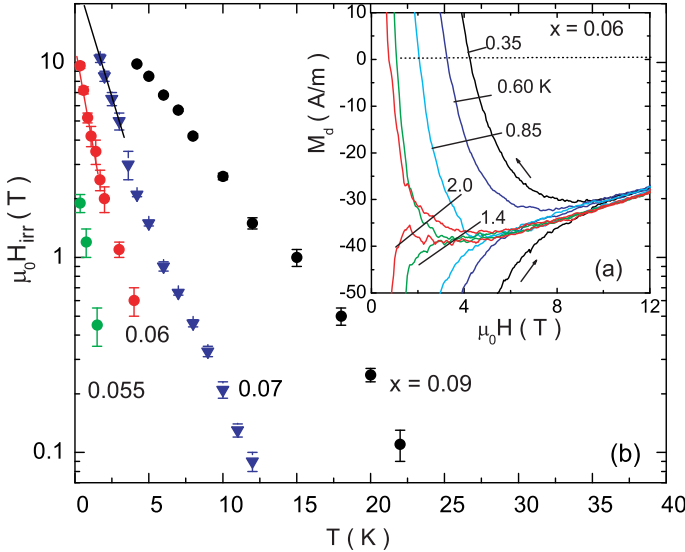


FIG. 3: The hysteretic curves in the vortex-solid phase of LSCO (Panel a) and the  $T$  dependence of the irreversibility field  $H_{irr}(T)$  in several samples (Panel b). Panel a displays hysteretic curves in Sample 06 at  $T$  from 0.35 to 2 K. Although the hysteretic segments for  $H < H_{irr}(T)$  are very strongly  $T$  dependent, the reversible segments above  $H_{irr}(T)$  are not. The latter match the  $T$ -constant profile shown in Fig. 2d. The  $T$  dependences of  $H_{irr}(T)$  in the samples 055, 06, 07 and 09 are shown in semilog scale in Panel b. At low  $T$ , the data approach Eq. 3. The steep decrease of the characteristic temperature  $T_0$  as  $x \rightarrow x_c$  implies a softening of the vortex solid ( $T_0 \sim 1$  K in 06).

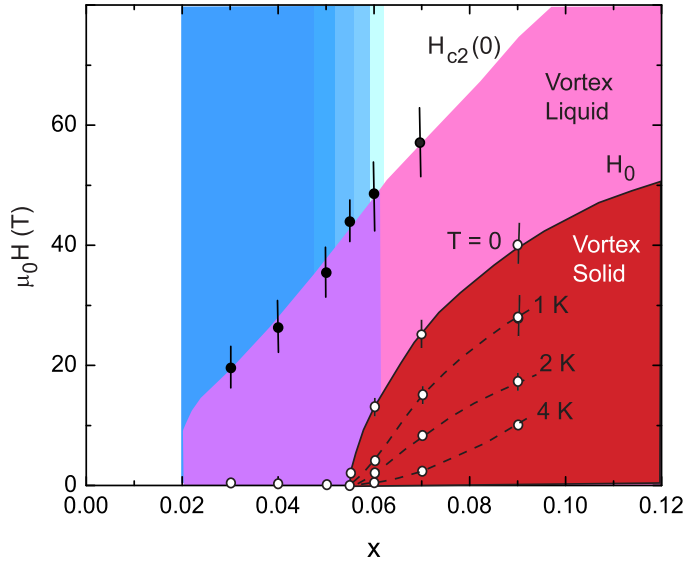


FIG. 4: The  $x$ - $H$  phase diagram of LSCO at low temperature, showing the vortex-solid state and the vortex-liquid state. The field  $H_0 = \lim_{T \rightarrow 0} H_{irr}$  falls steeply to zero as  $x \rightarrow x_c$  (solid curve). The dashed lines indicate the variation of  $H_{irr}(T)$  vs.  $x$  at fixed  $T$ , as indicated. By contrast, the depairing field  $H_{c2}(0)$  (closed circles) is nominally linear in  $x$ . Below  $x_c$ , the vortex liquid is stable and coexists with a growing magnetic background (graded shading).